

# DEEP DECOMPOSITION OF CIRCULARLY SYMMETRIC GABOR WAVELET FOR ROTATION-INVARIANT TEXTURE IMAGE CLASSIFICATION

Chaorong Li<sup>1,2</sup>, Yuanyuan Huang<sup>1</sup>

<sup>1</sup> University of Electronic Science and Technology of China

<sup>2</sup> Department of Computer Science and Information Engineering, Yibin University, China

## ABSTRACT

We propose Deep Decomposition of Circularly Symmetric Gabor Wavelet (DD-CSGW) for rotation-invariant texture image classification. Circularly Symmetric Gabor Wavelet (CSGW) is rotation-invariant tool for image analysis. However, CSGW has an obvious shortcoming: it extracts less discriminative information from image due to lack of directional selectivity. We make two contributions to improve the performance of CSGW: (1) We propose deep decomposition approach of CSGW to obtain more discriminative image information; (2) Because strong scale dependencies exist in the domain of CSGW, we use copula model to capture these scale dependencies. For classification, the energies of DD-CSGW and the parameters of copula model based on DD-CSGW are used as the features of texture, and SVM is utilized as the classifier. Experiments show that DD-CSGW obviously improves the performance of CSGW, and it is effective compared with the state-of-the-art rotation-invariant methods.

**Index Terms**— Texture classification, Circularly symmetric Gabor wavelet, Deep decomposition, Gaussian copula

## 1. INTRODUCTION

Image classification is an important research aspect in computer vision. A critical task for classification is how to effectively represent the given image using less discriminative information which is usually referred as the feature of image. In addition to feature representation, feature matching is needed to classify the images by means of the image features in database.

Dictionary learning [1, 2] and wavelet transform [3] are two efficient and interesting techniques of feature representation. Dictionary learning utilizes all the samples to train the dictionary, and then codes the image (or extracts the feature of image) according to the obtained dictionary. Compared with dictionary learning, wavelet transform directly uses wavelet basis, which is considered as a type of fixed dictionary, to

code image. Dictionary learning achieves greater flexibility, but it requires more complex computation. In addition to fast computation, wavelet transform has multiresolution property which is effective for analyzing the information content of images. In this paper, the proposed method absorbs multiresolution representations of wavelet transform, and uses a set of circularly symmetric Gabor filters (fixed dictionary) to extract the image features.

To most of the feature representation methods, the extracted features will be obviously different if the images are acquired at different directions. Therefore, designing a rotation-invariant method for image representation is still an important and challenging work. We know that wavelet transform based methods including discrete wavelet transform [4] and Gabor wavelet [5] are not rotation-invariant since different features would be produced at different subbands under the rotational condition. A few rotation-invariant techniques have been explored based on wavelet transform [6, 7]. Though, having the multiresolution property, wavelet based method (e.g. discrete wavelet and Gabor wavelet) has limited power for image representation.

In recent years, deep learning technique has been proposed [8, 9] which shows that the good internal image representation is hierarchical. Based on the theory of deep learning Bruna and Mallat [10] developed invariant scattering convolution networks which are constructed by implementing complex wavelet decomposition. Invariant scattering convolution networks obtained good performance of the image representation. Motivated by the above-mentioned methods, we propose the deep decomposition scheme for Circularly Symmetric Gabor Wavelet (CSGW), which is rotation-invariant filter designed by Porter and Canagarajah [11] based on Gabor filter. Furthermore, we capture the dependence structure at each layer by using copula model to improve the performance of CSGW.

## 2. CIRCULARLY SYMMETRIC GABOR WAVELET

2D Gabor filter takes a format of  $h(x, y) = g(x, y) \cdot e^{-2\pi j(Ux + Vy)}$ , where  $g(x, y)$  is Gaussian function, and  $(U, V)$  defines the position of the filter in the Fourier domain with a center frequency of  $W = \sqrt{U^2 + V^2}$ . 2D Gabor filter is not rotation-

This work is supported by the China Postdoctoral Science Foundation (No.2016M602675), the Foundation of the Central Universities in China (No.ZYGX2016J123), and the Project of Education Department of Sichuan Province (No.16ZA0328).

invariant since the sinusoidal grating ( $e^{-2\pi j(Ux+Vy)}$ ) of Gabor filter varies in only one direction. In order to obtain the rotation-invariance for Gabor filter, the complex sinusoidal grating can be modified to be circularly symmetric. Hence, Circularly Symmetric Gabor Filter (CSGF) is expressed as [11]

$$h_C(x, y) = \frac{1}{2\pi\sigma} e^{-1/2((x^2+y^2)/\sigma^2)} \cdot e^{-2\pi jW\sqrt{x^2+y^2}}, \quad (1)$$

where  $\frac{1}{2\pi\sigma} e^{-1/2((x^2+y^2)/\sigma^2)}$  is Gaussian function  $g(x, y)$ . Fig. 1 shows a CSGF in 3D space. We know that for obtaining the rotation-invariance, CSGF loses the directional selectivity compared to Gabor filter. By varying the scale factor  $\sigma$  of Gaussian function, we get the multiscale version of CSGF.

$$h_m(x, y) = \lambda^{-m} h_C(x', y'), \quad (2)$$

where  $x' = \lambda^{-m}x$ ,  $y' = \lambda^{-m}y$ ;  $\lambda^{-m}$  ( $m = 0, \dots, S-1$ ) denotes the scale parameter;  $S$  is the number of decomposition levels. Eq. (2) denotes a set of circularly symmetric filters with different scales (namely multiresolution property, see Fig. 2), called circularly symmetric Gabor wavelet (CSGW) in this paper.

### 3. DEEP DECOMPOSITION OF CSGW (DD-CSGW)

The purpose of designing CSGW is to obtain rotation-invariance for Gabor filters. However, without the directional selectivity as Gabor wavelet, CSGW will produce lesser discriminative information when applied to image analysis. Therefore, CSGW is relative less efficient for non-rotation image representation compared to Gabor wavelet. For obtaining more discriminative information, and then improving the performance for image representation, we propose a deep decomposition scheme base on CSGW, called DD-CSGW in this work. The deep decomposition refers to the iterative and hierarchical decompositions by using CSGW, which means that a coarser-scale subband can be continually decomposed into several finer-scale subbands by CSGF. It should be noted that the deep decomposition is not equal to the large number of scales decomposition. The performance of CSGW decomposition does not always been improved as the increase of scale number, and experiments show the best performance will be reached with five-scale decomposition[7]. Fig. 3 demonstrates the scheme of DD-CSGW with two layers. Given a image  $I(x, y)$ , the filtered output subbands by executing  $N$  layers DD-CSGW is expressed as

$$\begin{aligned} S[i] &= |h_m(x, y) * I(x, y)|, \\ S[i, j] &= |h_m(x, y) * s[i]|, \\ S[i, j, \dots, k, l] &= |h_m(x, y) * s[i, j, \dots, k]|, \end{aligned} \quad (3)$$

where  $i = 1, \dots, J_1$ ,  $j = 1, \dots, J_2$ ,  $k = 1, \dots, J_{N-1}$ ,  $l = 1, \dots, J_N$ ;  $J_i$  indicates the number of the scales in the  $i$ th layer decomposition. Sign  $|\cdot|$  indicates the module operator of

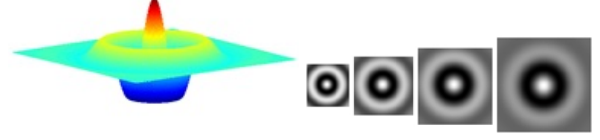


**Fig. 1.** CSGF in 3D space. **Fig. 2.** CSGW with four scales filters.

complex coefficients. In Eq. (3),  $S[i]$  and  $S[i, j]$  indicate decomposition subbands (or coefficients) in the first and the second layers. At each layer, we can use unified CSGW parameters including the decomposition level and the scale factor. The parameters of CSGW at each layer can be set differently. In fact, via experiments we observed that the performance of deep decomposition with different parameters at each layer is better than the performance with unified parameters.

## 4. IMAGE CLASSIFICATION USING DD-CSGW

### 4.1. Parameters of copula model on DD-CSGW

We use the parameters of copula model, which is a type of multivariate probability model, in the domain of DD-CSGW as the texture features. In fact, we can use univariate model such as Weibull distribution to independently fit each of the subbands. However our previous work [7] shows that there exist strong dependencies in the domain of CSGW. Hence, it can be deduce that the multivariate model which has the ability of capturing dependencies is more efficient than univariate model. The problem is we don't know what multivariate model is suitable for fitting the subbands of DD-CSGW. According to the characteristic of copula model, the scheme based on copula model is a good choice at this point. Here, we aim to establish several copula models and estimate the parameters of these copula models in the domain of DD-CSGW.

Recent year, copulas have been employed in wavelet domain and achieved success for image analysis[12]. Copula theorem states that if  $H(\mathbf{x})$  is a multivariate cumulative distribution function of a random vector  $\mathbf{x}(\mathbf{x} = [x_1, \dots, x_d])$ , then it can be expressed by the margins  $F_1(x_1), \dots, F_d(x_d)$  and a  $d$ -dimensional copula  $C: H(\mathbf{x}) = C(F_1(x_1), \dots, F_d(x_d))$ . The probability density function (pdf) of  $H$  is

$$h(\mathbf{x}) = c(F_1(x_1), \dots, F_d(x_d)) \cdot \prod_{i=1}^d f_i(x_i), \quad (4)$$

where  $f_i(x_i)$  and  $c$  are the pdfs of  $F_i(x_i)$  and copula  $C$  respectively. Eq (4) is called copula model in this work. It can be observed from copula model in (4) that if we know the univariate distributions of the subbands of DD-CSGW, then we can construct a multivariate model by using a proper copula function.

In this work we use Gaussian copula to capture the dependencies between the subbands of CSGW because the dis-

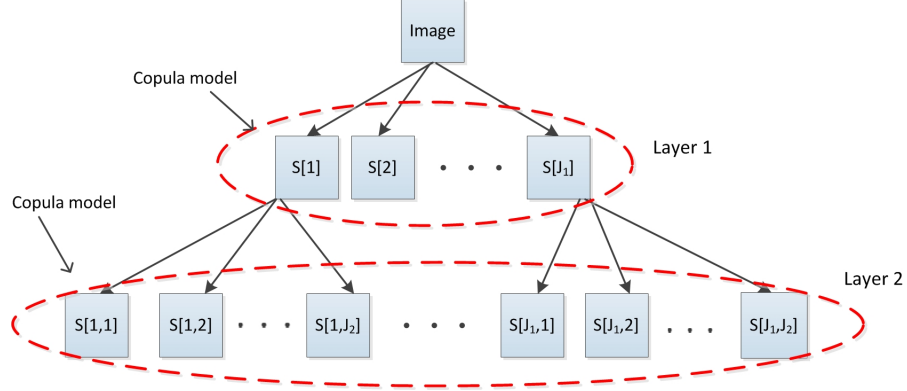


Fig. 3. DD-CSGW.

tribution of Gabor filter responses is approximate multivariate Gaussian. Gaussian copula shares some properties with Gaussian distribution such as symmetric shape since Gaussian copula is derived from Gaussian distribution. Therefore, it is feasible that Gaussian copula is used to capture the dependence structure between the subbands of CSGW. The pdf of Gaussian copula for a random vector  $\mathbf{u}(\mathbf{u} = [u_1, \dots, u_d])$  can be expressed as

$$c(\mathbf{u}) = |R|^{-1/2} \exp\left(-\frac{1}{2}\boldsymbol{\xi}^T(R^{-1} - I)\boldsymbol{\xi}\right), \quad (5)$$

where  $\boldsymbol{\xi} = [\xi_1, \dots, \xi_d]$ ,  $\xi_i = \Phi^{-1}(u_i)$ ,  $i = 1, \dots, d$ .  $\Phi$  is the standard normal distribution, and  $\Phi^{-1}$  denotes the quantile function corresponding to  $\Phi$ .  $R$  denotes the correlation matrix which is the parameter of Gaussian copula.

Since Weibull distribution can well fit the response of Gabor filter, we use Weibull as margins to model the subbands of DD-CSGW. The pdf of Weibull distribution is

$$f(x|\alpha, \beta) = \frac{\alpha}{\beta} \left(\frac{x}{\beta}\right)^{\alpha-1} e^{-\left(\frac{x}{\beta}\right)^\alpha}, \quad (6)$$

where  $\alpha$  and  $\beta$  are the shape parameter and scale parameter, respectively. The cumulative distribution function of Weibull distribution is given as follows

$$F(x|\alpha, \beta) = 1 - e^{-(x/\beta)^\alpha}. \quad (7)$$

To  $d$  subbands, then we will obtain  $f(x_i|\alpha_i, \beta_i)$  and  $F(x_i|\alpha_i, \beta_i)$ ,  $i = 1, \dots, d$ .

Based on (5), (6) and (7), the copula model of (4) can be constructed. The parameters of copula model including the  $R$  of Gaussian copula and  $\alpha_i$  and  $\beta_i$  of Weibull can be calculated by using two steps maximum likelihood estimation. The parameter set of a copula model is denoted by

$$\Omega = \{R, \alpha_1, \beta_1, \dots, \alpha_d, \beta_d\}. \quad (8)$$

The detailed description for constructing copula model and parameters estimation can be found in our previous work [13]. Simply, we construct one copula model at each layer of DD-CSGW (see Figure 3). To  $L$ -layer decomposition,  $L$  copula models and  $L$  parameter sets  $\{\Omega_i\}_1^L$  are to be produced.  $\{\Omega_i\}_1^L$  can be used as the features of texture image.

#### 4.2. Classification using SVM

We use Support Vector Machine (SVM) [14] as the classifier in our method since that SVM is good at processing high dimensional feature, and it has excellent computation efficiency compared with other learning-based classifiers such as neural networks. Given a training set of labeled samples  $\{\mathbf{X}_i, y_i\}_{i=1}^N$ , the goal of SVM is to obtain the following decision function

$$f(\mathbf{X}) = \sum_{i=1}^N \alpha_i y_i K(\mathbf{X}_i, \mathbf{X}) + b. \quad (9)$$

where  $\alpha_i$  are Lagrange multipliers;  $b$  is the offset to the origin;  $K(\mathbf{X}_i, \mathbf{X})$  is kernel function. To classification, the parameter of copula modes is used as the input of SVM. Because the parameter  $R$  is symmetric matrix, it should be translated into a vector, as following

$$R = \begin{bmatrix} 1 & r_{1,2} & \cdots & r_{1,d} \\ r_{2,1} & 1 & \cdots & r_{2,d} \\ \cdots & \cdots & \cdots & \cdots \\ r_{d,1} & r_{d,2} & \cdots & 1 \end{bmatrix} \rightarrow [r_{1,2} \quad \cdots \quad r_{d-1,d}] \quad (10)$$

Beside the parameters of copula model, we also use the norm-1 energy, norm-2 energy and standard deviation of DD-CSGW subband as the texture features. So the features

**Table 1.** Classification rate (%) on Outex database

Method	Outex_TC_00010	Outex_TC_00012	
		t184	horizon
LBP	97.84	85.76	84.54
LTP	98.2	93.59	89.42
CLBP	99.14	95.18	95.55
CLBC	99.38	94.98	95.51
DD-CSGW (Layer-1)	96.11	93.24	94.32
DD-CSGW (Layer-2)	97.86	97.84	98.38
DD-CSGW (Layer-3)	<b>99.64</b>	<b>98.82</b>	<b>98.91</b>

consist of two parts, denoted as follows

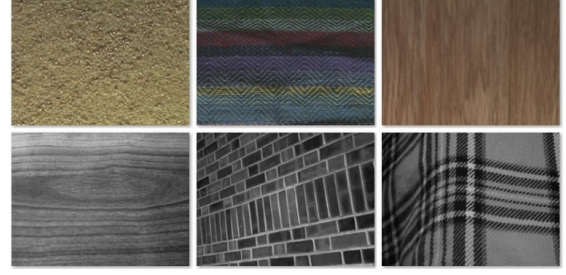
$$\begin{aligned}
 \mathbf{X} &= [\mathbf{X}_{CP}, \mathbf{X}_{es}], \\
 \mathbf{X}_{CP} &= [\cdots, \alpha_k^l, \beta_k^l, \cdots, r_{i,j}^l, \cdots]_{l=1}^L, \\
 \mathbf{X}_{en} &= [\cdots, m_k^l, e_k^l, s_k^l, \cdots]_{l=1}^L,
 \end{aligned} \tag{11}$$

where  $\mathbf{X}_{CP}$  indicates the parameter feature set of copula model;  $\mathbf{X}_{en}$  indicates the feature set including norm-1 energy features ( $m_k^l$ ,  $k$ th component at  $l$ th layer), norm-2 energy features ( $e_k^l$ ) and standard deviation features ( $s_k^l$ ).

## 5. EXPERIMENTS

To evaluate the performance of DD-CSGW, we carried out several classification experiments on Outex database [15] and UIUC database [16]. Some texture samples selected from two databases are shown in Figure 4. The proposed method is compared with several popular descriptors including LBP (local binary pattern) [17] and CLBP (complete LBP) [18], LTP (local ternary pattern) [19], and CLBC (complete local binary count)[20]. For making a fair comparison, the multi-scale scheme of these local descriptors is adopted. In our method, three-layer DD-CSGW decomposition is performed for the experiments; at first layer we use five-scale CSGW decomposition and three-scale CSGW decomposition is implemented at the other two layers; the filter parameters of CSGW are tuned to obtain best classification performance.

In Outex Database Outex\_TC\_00010 test suite and Outex\_TC\_00012 test suite were used. The two test suites contain the same 24 classes of textures, and 9 different rotation angles:  $0^\circ, 5^\circ, 10^\circ, 15^\circ, 30^\circ, 45^\circ, 60^\circ, 75^\circ$ , and  $90^\circ$ . To Outex\_TC\_00010, there are 4320 non-overlapping  $128 \times 128$  subimages. As to Outex\_TC\_00012, we used the illuminant “horizon” and “t184” (there are 9120 non-overlapping  $128 \times 128$  subimages). Our method achieved 99.64%, 98.82% and 98.91% for Outex\_TC\_00010, Outex\_TC\_00012 “t184” and

**Fig. 4.** Sample textures selected from Outex (first row) and UIUC (second row) texture databases.**Table 2.** Classification rate (%) on UIUC database

LBP	73.60
CLBP	90.60
DD-CSGW (Layer-3)	<b>90.80</b>

“horizon” respectively. It can be observed that deep decomposition scheme indeed improved the performance of CSGW. For example with three-layer decomposition, DD-CSGW (Layer-3) improved by roughly 5 percentage points than one-layer decomposition DD-CSGW (Layer-1). The classification rates are listed in Table 1 (the classification rates of other methods are cited from the corresponding original papers) in which we can see that DD-CSGW achieved much better results than other methods.

The UIUC texture database includes 25 classes with 40 images in each class, and the database contains materials imaged under significant viewpoint variations. The resolution of each image is  $640 \times 480$ . In this experiment, images were normalized into  $171 \times 128$ . We randomly chose 20 images from each class as the training set, and the remaining 20 images were used as test set. We implemented the multi-scale LBP and CLBP with three neighborhoods: ( $R=1, P=8$ ), ( $R=2, P=16$ ), and ( $R=3, P=24$ ). Experiments show that DD-CSGW obtains 90.80% classification rate which is close to the classification rate of multi-scale CLBP and is obviously higher than the classification rate of LBP.

## 6. CONCLUSION

DD-CSGW shows good performance for image representation compared to the state-of-the-art local descriptors. Deep decomposition is the highlight in this work, which remarkably improved the representation performance of CSGW and can be applied into other undecimated wavelet transform such as Gabor wavelet.

## 7. REFERENCES

- [1] Kreutz-Delgado Kenneth, F. Murray Joseph, D. Rao Bhaskar, Kjersti Engan, Lee Te-Won, and J. Sejnowski Terrence, "Dictionary learning algorithms for sparse representation," *Neural computation*, vol. 15, no. 2, pp. 349–396, 2003.
- [2] Yang Meng, Zhang Lei, Feng Xiangchu, and Zhang David, "Sparse representation based fisher discrimination dictionary learning for image classification," *International Journal of Computer Vision*, vol. 190, no. 3, pp. 209–232, 2014.
- [3] Gerlind Plonka, Stefanie Tenorth, and Armin Iske, "Optimally sparse image representation by the easy path wavelet transform," *International Journal of Wavelets, Multiresolution and Information Processing*, vol. 10, no. 01, pp. 1250007, 2012.
- [4] R Manthalkar, P.K Biswas, and B.N Chatterji, "Rotation and scale invariant texture features using discrete wavelet packet transform," *Pattern Recognition Letters*, vol. 24, no. 14, pp. 2455–2462, 2003.
- [5] S. Arivazhagana, L. Ganesanb, and S. Padam Priyala, "Texture classification using gabor wavelets based rotation invariant features," *Pattern Recognition Letters*, vol. 27, no. 16, pp. 1976–1982, 2006.
- [6] James DB Nelson and Nick G Kingsbury, "Enhanced shift and scale tolerance for rotation invariant polar matching with dual-tree wavelets," *Image Processing, IEEE Transactions on*, vol. 20, no. 3, pp. 814–821, 2011.
- [7] Chaorong Li, Guiduo Duan, and Fujinfujin Zhong, "Rotation invariant texture retrieval considering the scale dependence of gabor wavelet," *Image Processing, IEEE Transactions on*, vol. 24, no. 8, pp. 2344–2354, 2015.
- [8] Jason Weston, Frédéric Ratle, Hossein Mobahi, and Ronan Collobert, "Deep learning via semi-supervised embedding," in *Neural Networks: Tricks of the Trade*, pp. 639–655. Springer, 2012.
- [9] Yann LeCun, Yoshua Bengio, and Geoffrey Hinton, "Deep learning," *Nature*, vol. 521, no. 5, pp. 436–444, 2015.
- [10] Joan Bruna and Stéphane Mallat, "Invariant scattering convolution networks," *Pattern Analysis and Machine Intelligence, IEEE Transactions on*, vol. 35, no. 8, pp. 1872–1886, 2013.
- [11] R Porter and N Canagarajah, "Robust rotation-invariant texture classification: wavelet, gabor filter and gmrf based schemes," in *Vision, Image and Signal Processing, IEE Proceedings- IET*, 1997, vol. 144, pp. 180–188.
- [12] Nour-Eddine Lasmar and Yannick Berthoumieu, "Gaussian copula multivariate modeling for texture image retrieval using wavelet transforms," *Image Processing, IEEE Transactions on*, vol. 23, no. 5, pp. 2246–2261, 2014.
- [13] Chaorong Li, Yuanyuan Huang, and Lihong Zhu, "Color texture image retrieval based on gaussian copula models of gabor wavelets," *Pattern Recognition*, vol. 64, pp. 118–129, 2017.
- [14] Markos Papadonikolakis and Christos-Savvas Bouganis, "Novel cascade fpga accelerator for support vector machines classification," *IEEE transactions on neural networks and learning systems*, vol. 23, no. 07, pp. 1040–1052, 2012.
- [15] Timo Ojala, Topi Maenpaa, Matti Pietikainen, Jaakko Viertola, Juha Kyllonen, and Sami Huovinen, "Outex-new framework for empirical evaluation of texture analysis algorithms," in *Pattern Recognition, 2002. Proceedings. 16th International Conference on*. IEEE, 2002, vol. 1, pp. 701–706.
- [16] S Lazebnik, C Schmid, and J Ponce, "A sparse texture representation using local affine regions," *Pattern Analysis and Machine Intelligence IEEE Transactions on*, vol. 27, no. 8, pp. 1265–78, 2005.
- [17] Timo Ojala, Matti Pietikäinen, and Topi Mäenpää, "Multiresolution gray-scale and rotation invariant texture classification with local binary patterns," *Pattern Analysis and Machine Intelligence, IEEE Transactions on*, vol. 24, no. 7, pp. 971–987, 2002.
- [18] Zhenhua Guo, Lei Zhang, and David Zhang, "A completed modeling of local binary pattern operator for texture classification," *Image Processing, IEEE Transactions on*, vol. 19, no. 6, pp. 1657–1663, 2010.
- [19] Xiaoyang Tan and Bill Triggs, "Enhanced local texture feature sets for face recognition under difficult lighting conditions," *IEEE Transactions on Image Processing A Publication of the IEEE Signal Processing Society*, vol. 19, no. 6, pp. 1635–1650, 2010.
- [20] Y. Zhao, D. S. Huang, and W. Jia, "Completed local binary count for rotation invariant texture classification," *IEEE Transactions on Image Processing A Publication of the IEEE Signal Processing Society*, vol. 21, no. 10, pp. 4492, 2012.